

Epitaxial growth of Sn on Si(111): A direct atomic-structure determination of the $(2\sqrt{3}\times 2\sqrt{3})R30^\circ$ reconstructed surface

C. Törnevik, M. Hammar, N. G. Nilsson, and S. A. Flodström

Department of Physics, Materials Science, Royal Institute of Technology, S-100 44 Stockholm, Sweden

(Received 11 June 1991)

Scanning tunneling microscopy (STM) has been used to determine the surface atomic structure of Si(111) $(2\sqrt{3}\times 2\sqrt{3})$ -Sn. The topographic images show four resolved atoms in each $(2\sqrt{3}\times 2\sqrt{3})$ unit cell, and the structure is found to be onefold symmetric. Together with coverage measurements, the STM analysis implies that the reconstructed surface is an epitaxial Sn two-layer structure, where the atoms adopt a bonding configuration characteristic of α -Sn. A three-dimensional structure model, in accordance with the obtained results, is proposed.

Gray tin (α -Sn), the low-temperature semiconducting allotropic form of tin, forms sp^3 hybridization covalent bonds and crystallizes in the diamond structure, like the two other group-IV semiconducting elements silicon and germanium. Because of its zero band gap,¹ α -Sn has a great potential as a material in quantum-well structures with unique electronic properties.² A necessity for the realization of these structures is the formation of substrate-stabilized α -Sn films, stable above the normal α -Sn to β -Sn transition temperature (13.2°C). Such stabilization has been shown to be possible using various group IV,³ II-VI,⁴ or III-V (Ref. 5) semiconductor substrate surfaces. It is of fundamental importance to understand the origin of the stabilization mechanism. Determining the surface atomic and electronic structures of the early stages of epitaxial Sn growth on clean semiconductor surfaces, e.g., the Si(111) surface as chosen in this work, can provide essential information about the chemical behavior of Sn, and contribute to this understanding.

From low-energy electron-diffraction (LEED) and reflection high-energy electron-diffraction work on the Sn/Si(111) system, it is known that the deposition of Sn in the coverage range from one-third up to one monolayer [1 ML = 7.8×10^{14} atoms per cm^2 , the density of atoms in the ideal Si(111) surface plane] yields two coexisting surface reconstructions.^{3,6} One of these phases is a $(\sqrt{3}\times\sqrt{3})R30^\circ$ superstructure, for which the geometric and electronic structures are well known. It is induced by adsorption of $\frac{1}{3}$ of a ML of Sn atoms in the fourfold atop (T_4) site, i.e., above Si atoms in the second layer, as has been suggested from theoretical calculations⁷ and determined by experimental investigations using scanning tunneling microscopy⁸ (STM) and surface x-ray diffraction.⁹ Furthermore, angle-resolved ultraviolet photoelectron spectroscopy (ARUPS) and k -resolved inverse photoelectron spectroscopy (KRIPES) studies have shown that the surface electronic structure of the $(\sqrt{3}\times\sqrt{3})R30^\circ$ phase is very similar to the ones for the Si(111) $(\sqrt{3}\times\sqrt{3})$ -group III metal surfaces, and that the surface is metallic.^{10,11} The second phase is a $(2\sqrt{3}\times 2\sqrt{3})R30^\circ$ structure occurring for Sn coverages above $\frac{1}{3}$ ML, being complete at about 1 ML, and thus corresponding to a higher Sn content than the $(\sqrt{3}\times\sqrt{3})R30^\circ$ phase.³ A preliminary STM study by Nogami, Park, and Quate has suggested

that the $(2\sqrt{3}\times 2\sqrt{3})R30^\circ$ structure is twofold symmetric, their images indicating one elongated spot with a slight dip halfway along the long axis in each unit cell.⁸ It is known from ARUPS and KRIPES measurements that the $(2\sqrt{3}\times 2\sqrt{3})R30^\circ$ reconstructed surface is semiconducting, having at least one empty and two filled surface-state bands in the bulk band gap.¹¹ However, no geometric model has been proposed for this surface.

In this paper, we present scanning-tunneling-microscopy observations of the detailed atomic structure for the Si(111) $(2\sqrt{3}\times 2\sqrt{3})$ -Sn surface. Our topographic images, recorded both for filled and empty surface states, show four resolved atoms in each $(2\sqrt{3}\times 2\sqrt{3})R30^\circ$ unit cell. The observed atoms, which are assumed to be Sn, have equal intensities in pairs, showing that the structure has onefold symmetry. We propose a three-dimensional two-layer structure model for the $(2\sqrt{3}\times 2\sqrt{3})R30^\circ$ surface, based on determinations of the Sn atom positions relative to the Si substrate, and on measurements of Sn coverage, layer thickness, and separation between the observed atoms.

The experiments were performed in an ultrahigh-vacuum (UHV) system including a sample preparation and analysis chamber and a separate chamber for the STM (Omicron Vakuumphysik GmbH), both having a base pressure better than 1×10^{-10} Torr. The preparation chamber contains electron bombardment sample heating and ion sputtering equipment, evaporation sources, and LEED. Samples are easily transferred between the two chambers. Polished 0.5-mm-thick n -type Si(111) wafers, 0.004 Ωcm As-doped, were used for the experiments. After introduction of the samples into the vacuum, these were degassed at 700°C for several hours. Clean Si(111) (7×7) surfaces were produced by a short flash to 1100°C followed by annealing at 900°C for about 5 min. This procedure resulted in sharp (7×7) LEED patterns and STM images showing more than 1000-Å-large terraces with the (7×7) reconstruction. The images of the Si (7×7) surface were used to determine the orientation of the Si samples. Sn of 99.999% purity was evaporated from a tungsten filament source onto the clean Si(111) samples at a rate of 1 ML/min, as monitored by a quartz oscillator. The deposition was performed either onto samples which were kept at room temperature and afterwards

annealed to $\approx 600^\circ\text{C}$ for 2 min, or onto samples heated to $\approx 450^\circ\text{C}$. Prior to the STM investigation, the surface structure was checked with LEED. All STM images were taken at 1 nA tunneling current using tungsten tips, and both at positive and negative sample bias voltages, probing either unoccupied or occupied states.

Both the LEED patterns and the STM images showed that the Sn surface superstructures were most well grown when depositing onto heated samples, with large $(\sqrt{3} \times \sqrt{3})R30^\circ$ and $(2\sqrt{3} \times 2\sqrt{3})R30^\circ$ reconstructed domains and only a few disordered Sn islands. Surfaces with exclusively the $(\sqrt{3} \times \sqrt{3})R30^\circ$ or the $(2\sqrt{3} \times 2\sqrt{3})R30^\circ$ structure could be obtained by depositing a precise amount of Sn. No (7×7) reconstructed areas were seen in the images containing both the $(\sqrt{3} \times \sqrt{3})R30^\circ$ and the $(2\sqrt{3} \times 2\sqrt{3})R30^\circ$ reconstructions, i.e., for Sn coverages above $\frac{1}{3}$ ML. However, because of loss of Sn atoms from the surface during the deposition onto heated samples, the quartz oscillator could not be used to accurately determine the coverage for the $(2\sqrt{3} \times 2\sqrt{3})R30^\circ$ structure. Instead, the rate of increase of Sn coverage was estimated by measuring the evaporation time needed to get a complete $\frac{1}{3}$ ML $(\sqrt{3} \times \sqrt{3})R30^\circ$ reconstructed surface, which was investigated both with LEED and STM. This rate was then used to calculate the coverage when depositing enough Sn to obtain a distinct $(2\sqrt{3} \times 2\sqrt{3})$ LEED pattern and STM images showing surfaces entirely covered with the $(2\sqrt{3} \times 2\sqrt{3})R30^\circ$ phase. In this way the Sn coverage for this reconstruction was found to be between 0.9 and 1.2 ML.

Figure 1 is a $(330 \times 280)\text{-}\text{\AA}^2$ topographic image taken at +1.5 V sample voltage, showing a single domain of the Si(111) $(2\sqrt{3} \times 2\sqrt{3})$ -Sn surface. Each unit cell of the hexagonal structure displays four protrusions which in pairs have equal intensities, showing that the structure has onefold symmetry. The pairs are oriented in a $\langle \bar{1}10 \rangle$ type direction and three different orientations of the structure are observed in separate domains in several images, explaining the threefold symmetry of the LEED pattern.

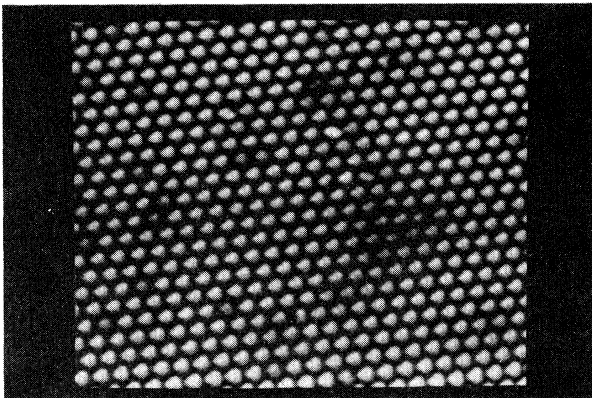


FIG. 1. A $(330 \times 280)\text{-}\text{\AA}^2$ STM topographic image of the Si(111) $(2\sqrt{3} \times 2\sqrt{3})$ -Sn surface, taken with a sample voltage of +1.5 V at a constant current of 1.0 nA. The full gray scale range corresponds to a height difference of 2.5 \AA .

The boundaries between the domains are oriented in $\langle \bar{1}\bar{1}2 \rangle$ type directions. Assuming that the four topographic maxima in each $(2\sqrt{3} \times 2\sqrt{3})R30^\circ$ unit cell are single Sn atoms, these correspond to a coverage of $\frac{1}{3}$ ML. Consequently, between 0.6 and 0.9 ML of Sn atoms are not observed in the images, indicating that the structure contains a second Sn layer beneath the layer observed by STM.

Some of the different types of defects observed for the $(2\sqrt{3} \times 2\sqrt{3})R30^\circ$ structure are seen in the image in Fig. 1. From one up to all four atoms in a unit cell can be missing. The lateral positions of the remaining atoms in a unit cell do not change when an atom is absent, which indicates that there are no or only weak direct interactions between the surface layer atoms. However, the intensities (heights) of the surrounding atoms are affected by a vacancy, an effect which is likely to be electronic.

Figure 2 shows $(45 \times 45)\text{-}\text{\AA}^2$ high-resolution tunneling images of the same area of the $(2\sqrt{3} \times 2\sqrt{3})R30^\circ$ reconstructed surface, acquired at +1.5 and -1.5 V sample bias. When tunneling into empty surface states (+1.5 V), the four atoms in each unit cell are clearly resolved. The direction from the lower to the higher atom-pair center is of a $\langle \bar{1}\bar{1}2 \rangle$ type, and the intensity difference between the brighter and the weaker spots corresponds to a height difference of $0.5 \pm 0.2 \text{\AA}$. In the image obtained by tunneling out of filled states (-1.5 V) the height difference is about 0.4 \AA larger. This suggests that there is both a geometric and an electronic height difference between the two pairs in the topmost surface layer. For images acquired both at positive and at negative sample voltages, the separation between the intensity maxima for the two lower atoms is $4.2 \pm 0.2 \text{\AA}$, and between a high and a low atom $5.3 \pm 0.2 \text{\AA}$. The lower atoms are well resolved also in the filled state images, while the higher atoms appear to be closer to each other, the spacing between the intensity maxima changing from $4.6 \pm 0.2 \text{\AA}$ in the empty state images to $3.7 \pm 0.2 \text{\AA}$ when tunneling out of filled states.

In order to obtain the registration relative to the silicon bulk lattice for the four atoms visible in each $(2\sqrt{3} \times 2\sqrt{3})R30^\circ$ unit cell, Sn was deposited in the range between $\frac{1}{3}$ and 1 ML, giving surfaces with coexisting

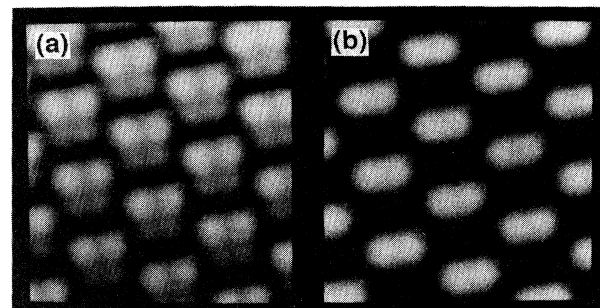


FIG. 2. $(45 \times 45)\text{-}\text{\AA}^2$ tunneling images of the same few unit cells of the Si(111) $(2\sqrt{3} \times 2\sqrt{3})$ -Sn surface, acquired with a sample voltage of (a) +1.5 V and (b) -1.5 V at a constant current of 1.0 nA. The total corrugation in the images is $2.0 \pm 0.2 \text{\AA}$.

$(\sqrt{3}\times\sqrt{3})R30^\circ$ and $(2\sqrt{3}\times2\sqrt{3})R30^\circ$ reconstructed areas. In the STM images of these samples, $(2\sqrt{3}\times2\sqrt{3})R30^\circ$ phase islands are seen on the $(\sqrt{3}\times\sqrt{3})\times R30^\circ$ reconstructed surface. Since the $(\sqrt{3}\times\sqrt{3})\times R30^\circ$ adatoms are known to lie in T_4 positions,⁸ which was confirmed from low Sn coverage samples with (7×7) and $(\sqrt{3}\times\sqrt{3})R30^\circ$ areas, the registration for the $(2\sqrt{3}\times2\sqrt{3})R30^\circ$ phase protrusions can be determined from these images.¹² Figure 3(a) shows an image obtained after deposition of ≈ 0.5 ML of Sn, with a domain boundary between the two different reconstructions. Grid lines aligned to the $(\sqrt{3}\times\sqrt{3})R30^\circ$ pattern are extrapolated across the domain boundary. An examination of this image shows that the high atoms are lying close to positions above atoms in the second Si layer (above T_4 sites), and the low atoms close to positions above atoms in the fourth Si layer, i.e., above threefold hollow sites (H_3 sites). This position identification is shown in Fig. 3(b).

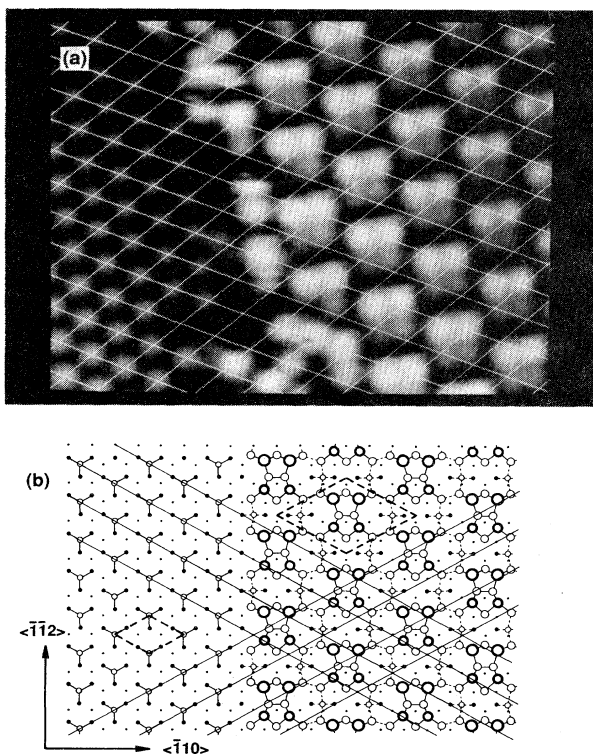


FIG. 3. (a) Topographic image of a phase boundary between $(\sqrt{3}\times\sqrt{3})R30^\circ$ (left side) and $(2\sqrt{3}\times2\sqrt{3})R30^\circ$ (right side) structures. A $(\sqrt{3}\times\sqrt{3})R30^\circ$ unit-cell grid is aligned to the adatom positions (T_4 sites), and extrapolated across the phase boundary, in order to determine the registration of the top atoms in the $(2\sqrt{3}\times2\sqrt{3})R30^\circ$ structure. (b) Topview atomic diagram showing the identification of the positions of the four top atoms in the $(2\sqrt{3}\times2\sqrt{3})R30^\circ$ structure, and the proposed structural model. The sizes of the $(\sqrt{3}\times\sqrt{3})R30^\circ$ and $(2\sqrt{3}\times2\sqrt{3})R30^\circ$ unit cells are indicated. Solid circles represent Si atoms and open circles represent Sn atoms. Larger circles correspond to atoms in layers closer to the surface. See text for further details.

The distance between the considered H_3 and T_4 sites is 4.43 Å, about 0.9 Å less than the measured separation between a high and a low atom. However, the corresponding distance for an ideal α -Sn(111) surface is 5.30 Å, indicating that the atoms in a possible second Sn layer tend to take positions characteristic of α -Sn. The average separation between the two atoms in a pair is 4.2 Å, a value approximately halfway between those for the distances between two T_4 (or two H_3 sites) in Si(111) and α -Sn(111).

The domain boundaries between the $(2\sqrt{3}\times2\sqrt{3})R30^\circ$ islands and the $(\sqrt{3}\times\sqrt{3})R30^\circ$ areas run preferentially in $\langle 1\bar{1}2 \rangle$ type directions, and there is a step between the two phases, the $(2\sqrt{3}\times2\sqrt{3})R30^\circ$ top atoms being 2.1 ± 0.1 Å higher than the $(\sqrt{3}\times\sqrt{3})R30^\circ$ adatoms. In several images the growth of the $(2\sqrt{3}\times2\sqrt{3})R30^\circ$ islands seems to originate from less-ordered Sn islands. A second type of step is seen in some images, where the $(2\sqrt{3}\times2\sqrt{3})R30^\circ$ phase top atoms are 1.0 ± 0.1 Å lower than the $(\sqrt{3}\times\sqrt{3})R30^\circ$ phase adatoms. The sum of heights for the two different steps is ≈ 3.1 Å, close to the thickness of a Si(111) double layer (3.13 Å), implying that the smaller step is the result of the start of growth of $(2\sqrt{3}\times2\sqrt{3})R30^\circ$ islands at a Si bulk step. Accordingly, the 2.1-Å step has to be the difference in thickness between the two superstructures. The $(\sqrt{3}\times\sqrt{3})R30^\circ$ adatoms are known to sit 1.44 Å above the Si surface,^{7,9} meaning that the thickness of the $(2\sqrt{3}\times2\sqrt{3})R30^\circ$ structure is about 3.5 Å. This value is fairly close to 3.74 Å, the thickness of an α -Sn(111) double layer. Assuming that Sn atoms bond on top of the Si atoms, the distance to the Si(111) surface plane will be equal to the Si-Sn bond length, 2.57 Å, obtained as the sum of the covalent radii, which is 0.24 Å less than the bond length in bulk α -Sn (2.81 Å). Consequently, the thickness of an adsorbed Sn double layer should be less than 3.74 Å, near the observed value 3.5 Å. The assumption of bonding of Sn atoms on top of Si atoms is supported by LEED and photoemission yield spectroscopy work on the Si(111)(2×1) cleavage surface.¹³ Our results indicate that the Sn atoms in the $(2\sqrt{3}\times2\sqrt{3})R30^\circ$ overlayer tend to form a bonding configuration typical of α -Sn, i.e., covalent bonds and fourfold coordination, and that the structure is an incomplete α -Sn(111) double layer. This room-temperature stabilization of the properties characteristic of the semiconducting form of Sn, resulting in a local α -Sn(111) double-layer structure, has to be promoted by the clean Si(111) substrate. However, the formation of a complete epitaxial α -Sn(111) double layer is not possible because of the large lattice mismatch (20%) between Si and α -Sn.

In Fig. 3(b) we propose a three-dimensional structural model for the Si(111)($2\sqrt{3}\times2\sqrt{3}$)-Sn surface, which is based on the STM results and the assumption that the overlayer consists only of Sn, with an abrupt interface to the substrate and without intermixing of Sn and Si atoms. This assumption is founded on the very small bulk solubility of Sn in Si, and on studies with other techniques which have demonstrated the abrupt character of the Sn/Si(111) interface.^{3,13} The model consists of Sn dimers arranged in a $(2\sqrt{3}\times2\sqrt{3})$ pattern, the dimer atoms bonding in top

positions to Si atoms. Around each dimer are six Sn atoms, also bonding in top positions but somewhat displaced outwards to form a local structure with in-plane distances close to those characteristic of α -Sn(111), 4.59 Å. Each of these eight Sn atoms in the unit cell passivate one Si dangling bond. Two other Sn atoms are postulated to be placed in bridge sites to eliminate the remaining Si dangling bonds. Finally, four Sn adatoms per $(2\sqrt{3} \times 2\sqrt{3})R30^\circ$ unit cell, corresponding to the four atoms observed in the STM images, bond in the obtained hollow sites next to the dimers, two with a correct stacking and two with a stacking fault with respect to the Si bulk lattice. This difference in bonding sites for the adatoms may be an explanation of the height difference in the topographs. Lines between atoms in the figure symbolize bonds. Further possible bonds, besides the dimer and adatom bonds, which make additional Sn atoms obtain four-fold coordination, are marked with dashed lines. Each unit cell will then contain six dangling Sn bonds, four at the adatoms and two in the second layer. The Sn coverage for the proposed model is 1.17 ML. This value, as well as the adatom separations and the overlayer thickness, is in good agreement with the measurements. The structure in this model can be seen as consisting of locally complete α -Sn(111) double-layer subunits, where the deviations from ideal bonding angles are rather small. However, additional relaxations of the Si atoms in the first few layers, minimizing the elastic strain, are likely to exist. The building blocks in our structural model are similar to the ones that are present on various reconstructed semiconductor surfaces.¹⁴ For example, the dimers and the stacking fault in this model are analogous to those in the dimer-adatom-stacking fault (DAS) model for the Si(111)(7×7) surface.¹⁵ As for the Si(7×7) surface, a possible explanation of the electronic height difference be-

tween the two different pairs of adatoms is the occurrence of a charge transfer from the side of the unit cell containing the correctly stacked adatoms to the other side.¹⁶ In addition, a simple explanation of the semiconducting nature of the surface can be obtained by counting the total number of valence electrons per unit cell for the $(2\sqrt{3} \times 2\sqrt{3})R30^\circ$ structure, including the 12 Si dangling bonds.¹¹ This yields an even number of electrons, predicting the structure to be semiconducting.

To summarize, we have studied the atomic surface topography of Si(111)($2\sqrt{3} \times 2\sqrt{3}$)-Sn under UHV conditions by STM. The images show large well-grown areas of the structure, for which the Sn coverage was determined to be between 0.9 and 1.2 ML. High-resolution topographic images reveal that the structure is onefold symmetric, and four atoms are resolved in each unit cell. Three possible orientations of the structure on the surface explain the threefold symmetry observed by LEED. We have determined the overlayer thickness and the registration for the observed atoms relative to the Si bulk lattice. From the STM data it is concluded that the structure consists of two layers of Sn, where the atoms are believed to adopt a bonding configuration characteristic of α -Sn, indicating that the clean Si(111) surface can stabilize the semiconducting nature of thin Sn layers at room temperature. A three-dimensional structural model is proposed for the reconstruction, comprised of similar building blocks as are used in the DAS model for the Si(111)(7×7) surface.

This work was supported by the Swedish Natural Science Research Council. We wish to thank Dr. J. M. Nicholls for important contributions at the start of the project.

¹S. Groves and W. Paul, Phys. Rev. Lett. **11**, 194 (1963).

²C. H. L. Goodman, IEE Proc. **129**, 189 (1982).

³T. Ichikawa, Surf. Sci. **140**, 37 (1984).

⁴M. T. Asom, A. R. Kortan, L. C. Kimerling, and R. C. Farrow, Appl. Phys. Lett. **55**, 1439 (1989).

⁵J. L. Reno and L. L. Stephenson, Appl. Phys. Lett. **54**, 2207 (1989).

⁶P. J. Estrup and J. Morrison, Surf. Sci. **2**, 465 (1964).

⁷S. K. Ramchurn, D. M. Bird, and D. W. Bullett, J. Phys. Condens. Matter **2**, 7435 (1990).

⁸J. Nogami, S. I. Park, and C. F. Quate, J. Vac. Sci. Technol. A **7**, 1919 (1989).

⁹K. M. Conway, J. E. Macdonald, C. Norris, E. Vlieg, and J. F. van der Veen, Surf. Sci. **215**, 555 (1989).

¹⁰T. Kinoshita, S. Kono, and T. Sagawa, Phys. Rev. B **34**, 3011 (1986).

¹¹T. Kinoshita, H. Ohta, Y. Enta, Y. Yaegashi, S. Suzuki, and S. Kono, Jpn. J. Appl. Phys. **56**, 4015 (1987).

¹²R. J. Wilson and S. Chiang, J. Vac. Sci. Technol. A **6**, 398 (1988).

¹³A. Taleb-Ibrahimi, C. A. Sebenne, F. Proix, and P. Maigne, Surf. Sci. **163**, 478 (1985).

¹⁴See, for example, G. V. Hansson, and R. I. G. Uhrberg, Surf. Sci. Rep. **9**, 197 (1988).

¹⁵K. Takayanagi, Y. Tanishiro, M. Takahashi, and S. Takahashi, J. Vac. Sci. Technol. A **3**, 1502 (1985).

¹⁶R. D. Meade and D. Vanderbilt, Phys. Rev. B **40**, 3905 (1989).

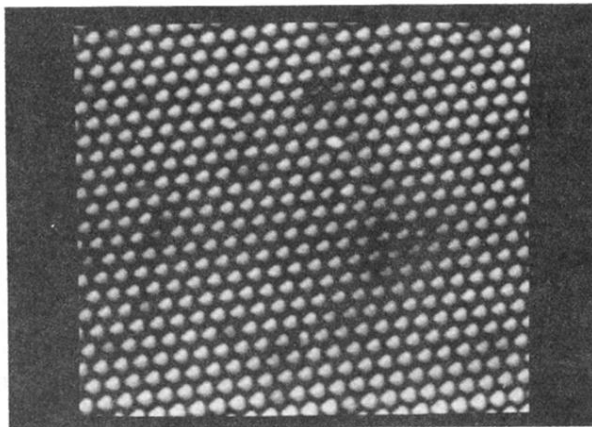


FIG. 1. A $(330 \times 280)\text{-\AA}^2$ STM topographic image of the $\text{Si}(111)(2\sqrt{3} \times 2\sqrt{3})\text{-Sn}$ surface, taken with a sample voltage of +1.5 V at a constant current of 1.0 nA. The full gray scale range corresponds to a height difference of 2.5 Å.

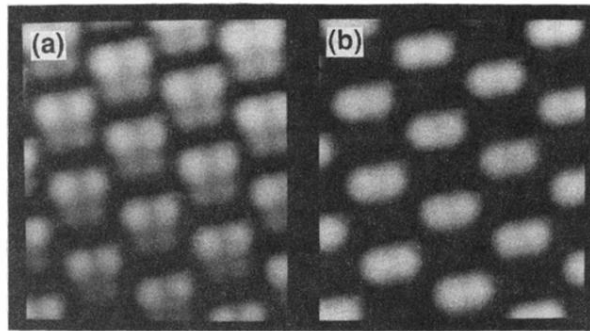


FIG. 2. $(45 \times 45)\text{-}\text{\AA}^2$ tunneling images of the same few unit cells of the $\text{Si}(111)(2\sqrt{3} \times 2\sqrt{3})\text{-Sn}$ surface, acquired with a sample voltage of (a) $+1.5\text{ V}$ and (b) -1.5 V at a constant current of 1.0 nA . The total corrugation in the images is $2.0 \pm 0.2\text{ \AA}$.

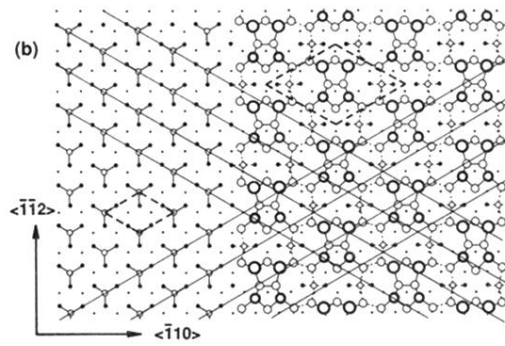
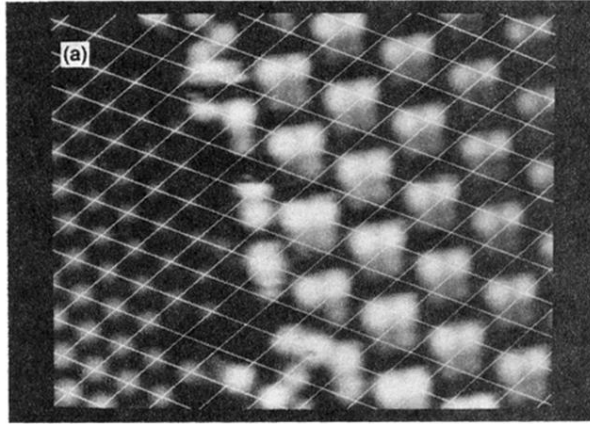


FIG. 3. (a) Topographic image of a phase boundary between $(\sqrt{3} \times \sqrt{3})R30^\circ$ (left side) and $(2\sqrt{3} \times 2\sqrt{3})R30^\circ$ (right side) structures. A $(\sqrt{3} \times \sqrt{3})R30^\circ$ unit-cell grid is aligned to the adatom positions (T_4 sites), and extrapolated across the phase boundary, in order to determine the registration of the top atoms in the $(2\sqrt{3} \times 2\sqrt{3})R30^\circ$ structure. (b) Topview atomic diagram showing the identification of the positions of the four top atoms in the $(2\sqrt{3} \times 2\sqrt{3})R30^\circ$ structure, and the proposed structural model. The sizes of the $(\sqrt{3} \times \sqrt{3})R30^\circ$ and $(2\sqrt{3} \times 2\sqrt{3})R30^\circ$ unit cells are indicated. Solid circles represent Si atoms and open circles represent Sn atoms. Larger circles correspond to atoms in layers closer to the surface. See text for further details.